Supporting Information for:

Planar Dy_3+Dy_3 clusters: Design, structures and axial ligands perturbed magnetic dynamics

Experimental Section

General. All starting materials were of A.R. Grade and were used as commercially obtained without further purification. 4,6-dihydrazinopyrimidine was prepared according to a previously published method.[1]

Elemental analyses for C, H, and N were carried out on a Perkin-Elmer 2400 analyzer. Fourier transform IR (FTIR) spectra were recorded with a Perkin-Elmer FTIR spectrophotometer using the reflectance technique (4000−300 cm^{-1}). Samples were prepared as KBr disks. All magnetization data were recorded on a Quantum Design MPMS-XL7 SQUID magnetometer equipped with a 7 T magnet. The variable-temperature magnetization was measured with an external magnetic field of 1000 Oe in the temperature range of 1.9−300 K. The experimental magnetic susceptibility data are corrected for the diamagnetism estimated from Pascal's tables and sample holder calibration.

Synthesis of the Complex Dy_6−SCN

$[Dy_6L_2(\mu_3\text{-}OH)_4(\mu_2\text{-}OH)_2(SCN)_8(H_2O)_4]\cdot 6CH_3CN\cdot 2CH_3OH\cdot H_2O$ (**Dy_6−SCN**).

4,6-dihydrazinopyrimidine (0.1 mmol) was dissolved in a mixture of methanol and acetonitrile (1:2, 15 mL), and then o-vanillin (0.2 mmol) was added to the mixture. The reaction mixture was stirred for 5 min. Then, triethylamine (0.3 mmol) and $Dy(SCN)_3\cdot 6H_2O$ (0.2 mmol) were added after 5 min successively. The reaction mixture was stirred at room temperature for 4 h and the resultant solution was left unperturbed to allow for slow evaporation of the solvent. Yellow single crystals of complex **Dy_6−SCN** were obtained after two days. Yield: 20 mg, (21.8 %, based on the metal salt). Elemental analysis (%) calcd for $C_{31}H_{35.25}Dy_3N_{13.25}O_{10.5}S_4$: C, 27.04, H, 2.58, N, 13.48; found C, 27.08, H, 2.60, N, 13.46. IR (KBr, cm^{-1}): 3277 (w), 3204 (w), 2045 (s), 1617 (s), 1509 (m), 1503 (m), 1484 (m), 1460 (s), 1423 (m), 1320 (s), 1292 (m), 1218 (s), 1197 (s), 1167 (w) 1115 (s), 1078 (m), 1009 (m) 750 (m), 737 (s).

Synthesis of the Complex Dy_6−NO_3

$[Dy_6L_2(\mu_3\text{-}OH)_4(\mu_2\text{-}OH)_2(NO_3)_6(H_2O)_6]\cdot 2NO_3\cdot 10H_2O$ (**Dy_6−NO_3**).

4,6-dihydrazinopyrimidine (0.1 mmol) was dissolved in a mixture of methanol and acetonitrile (1:2, 15 mL), and then o-vanillin (0.2 mmol) was added to the mixture. The reaction mixture was stirred for 5 min. Then, triethylamine (0.3 mmol) and $Dy(NO_3)_3\cdot 6H_2O$ (0.1 mmol) were added after 5 min successively. The reaction mixture was stirred at room temperature for 4 h and the resultant solution was left unperturbed to allow for slow evaporation of the solvent. Yellow single crystals of complex **Dy_6−NO_3** were obtained after a week. Yield: 11 mg, (24.9 %, based on the metal salt). Elemental analysis (%) calcd for $C_{44}H_{54}Dy_6N_{16}O_{54}$: C, 19.97, H, 2.06, N, 8.47; found C, 19.95, H, 2.07, N, 8.46. IR (KBr, cm^{-1}): 3428 (m), 3191 (m), 1620 (s), 1517 (w), 1460 (m), 1427 (m), 1322 (s), 1290 (m), 1219 (m), 1199 (m), 1116 (w), 1079 (w), 1044 (w), 946 (w), 857 (w), 815 (w), 780 (w), 735 (m).

X-ray Crystallography.

Crystallographic data and refinement details are given in Table S3. Suitable single crystal of **Dy_6−SCN** and **Dy_6−NO_3** were selected for single-crystal X-ray diffraction analysis. Crystallographic data were collected at 296(1) and 113(1) K on a Bruker ApexII CCD diffractometer and with graphite monochromated Mo Kα radiation (λ = 0.71073 Å). The structures were solved by direct methods and refined by the full-matrix least-squares method based on F^2 with anisotropic thermal parameters for all non-hydrogen atoms by using the SHELXS (direct methods) and refined by SHELXL (full matrix least-squares techniques) in the Olex2 package.[2] The locations of Dy atom were easily determined, and O, N, C and S atoms were subsequently determined from the difference Fourier maps. Anisotropic thermal parameters were assigned to all non-hydrogen atoms. The H atoms were introduced in calculated positions and refined with a fixed geometry with respect to their carrier atoms. CCDC 1419275 (**Dy_6−SCN**) and 1419276 (**Dy_6−NO_3**) contain the supplementary crystallographic data for this paper. These data can be obtained free of charge from the Cambridge Crystallographic Data Centre via www.ccdc.cam.ac.uk/data_request/cif.

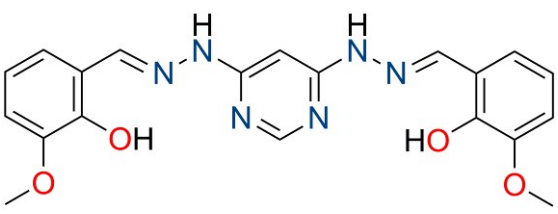

Scheme S1. Structure of the H_2L ligand.

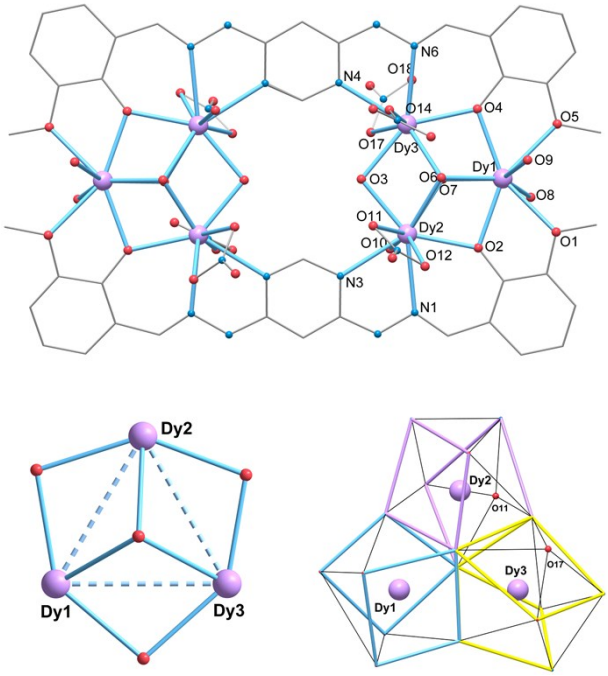

Fig. S1 (top) Partially labeled Dy_3 structures of complex **Dy_6−NO_3** with H atoms omitted for clarity. Color scheme: pink, Dy; red, O; blue, N. (bottom left) Overall central core for **Dy_6−NO_3**. (bottom right) Coordination polyhedra observed in **Dy_6−NO_3**: square-antiprismatic environment for Dy1 and mono-capped square antiprism geometries for Dy2/Dy3.

Table S1. Dy^{III} geometry analysis of **Dy_6−SCN** by SHAPE 2.1 software.

Dy^{III}	Triangular dodecahedron (D_{2d})	Square antiprism (D_{4d})	Biaugmented trigonal prism (C_{2v})	Biaugmented trigonal prism J50 (C_{2v})	Snub diphenoid J84 (D_{2d})
Dy^{III}(1)	1.930	**1.382**	2.786	3.322	5.021
Dy^{III}(2)	**0.840**	3.005	2.315	2.596	2.057
Dy^{III}(3)	**1.008**	2.539	1.877	2.342	2.102

Table S2. Dy^{III} geometry analysis of **Dy_6−NO_3** by SHAPE 2.1 software.

Dy^{III}	Triangular dodecahedron (D_{2d})	Square antiprism (D_{4d})	Biaugmented trigonal prism (C_{2v})	Biaugmented trigonal prism J50 (C_{2v})	Snub diphenoid J84 (D_{2d})
Dy^{III}(1)	1.982	**1.418**	2.884	3.525	4.981
	Spherical capped square antiprism (C_{4v})	Spherical tricapped trigonal prism (D_{3h})	Capped square antiprism J10 (C_{4v})	Tricapped trigonal prism J51 (D_{3h})	Muffin (C_s)
Dy^{III}(2)	**1.884**	2.081	2.410	2.532	2.505
Dy^{III}(3)	**1.599**	2.220	2.436	2.514	2.318

Table S3. Crystal data and structure refinement for complexes **Dy_6−NO_3** and **Dy_6−SCN**.

Compound	**Dy_6−NO_3**	**Dy_6−SCN**
Empirical formula	$C_{44}H_{54}Dy_6N_{16}O_{54}$	$C_{31}H_{35.25}Dy_3N_{13.25}O_{10.5}S_4$
Fw (g/mol)	2654.03	1377.21
Temperature/K	296.15	113.1500
Crystal system	Triclinic	Monoclinic
Space group	Pī	C2/c
a/Å	10.7890(11)	40.411(8)
b/Å	12.7071(13)	11.713(2)
c/Å	16.9727(18)	30.558(6)
α/°	100.954(2)	90
β/°	100.243(2)	129.65(3)
γ/°	109.293(2)	90
V/Å^3	2082.3(4)	11137(5)
Z	1	8
ρ_{calc} (g/cm^3)	2.117	1.643
F(000)	1262.0	5280.0
R_{int}	0.0309	0.0775
R_1 wR_2 [$I >= 2\sigma(I)$]	0.0451, 0.1270	0.0741, 0.1806
R_1 wR_2 [all data]	0.0599, 0.1393	0.0955, 0.1932
GoF	1.047	1.096

Table S4. The corresponding distances and angles of Dy_3 triangle in complexes **Dy_6−NO_3** and **Dy_6−SCN**.

	Dy_6−NO_3	**Dy_6−SCN**
Dy1−Dy2	3.523 Å	3.540 Å
Dy1−Dy3	3.512 Å	3.534 Å
Dy2−Dy3	3.519 Å	3.505 Å
Dy1−Dy2−Dy3	59.835°	60.206°
Dy2−Dy3−Dy1	60.142°	60.390°
Dy3−Dy1−Dy2	60.023°	59.403°
Dihedral Angle	0°	5.153°
Distance between two Dy_3 plans	0.2361 Å	−

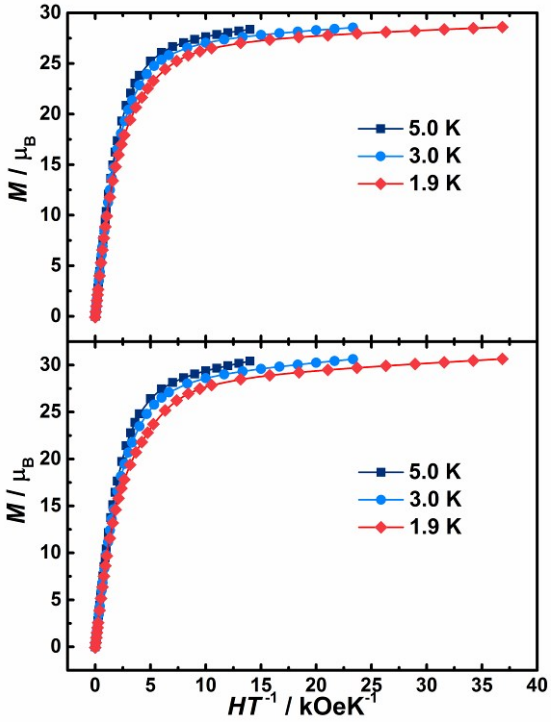

Fig. S2 *M* vs. *H*/*T* plots for complexes **Dy_6–SCN** (top) and **Dy_6–NO_3** (bottom) at various temperatures between 1.9 and 5 K.

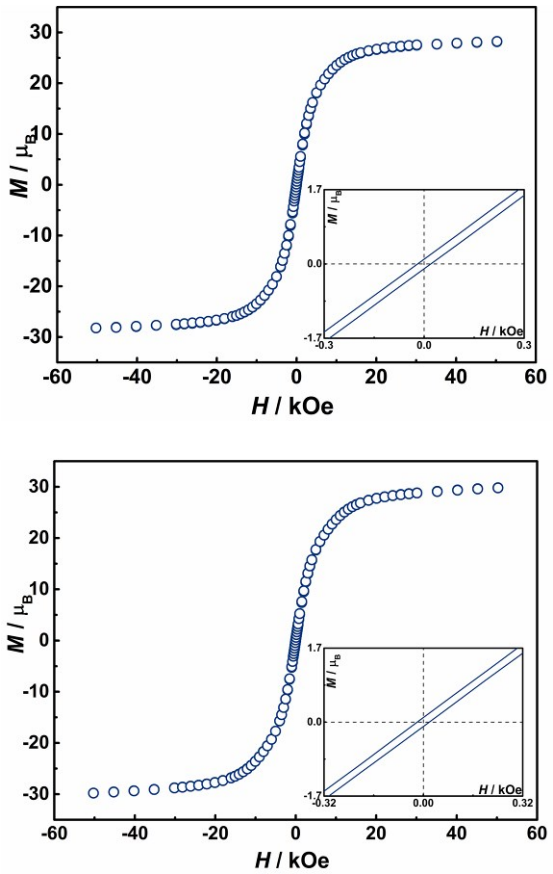

Fig. S3 Hysteresis loop for complexes **Dy_6−SCN** (top) and **Dy_6−NO_3** (bottom) at 1.9 K, showing a narrow hysteresis for **Dy_6−SCN** and **Dy_6−NO_3**, respectively. (Inset figures).

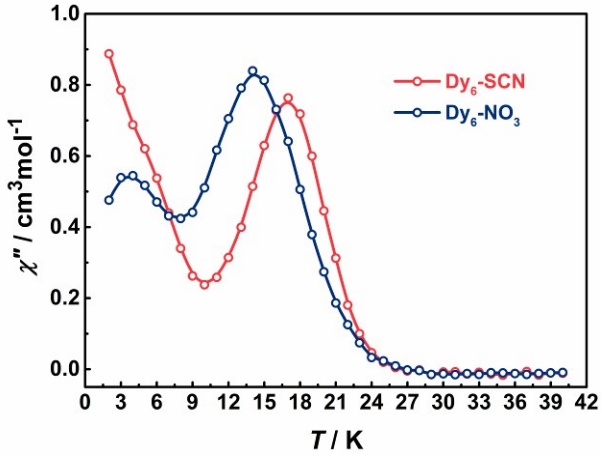

Fig. S4 Temperature dependence of the (χ'') ac susceptibility components under zero dc-field and at 1000 Hz ac frequency for **Dy_6−SCN** and **Dy_6−NO_3**.

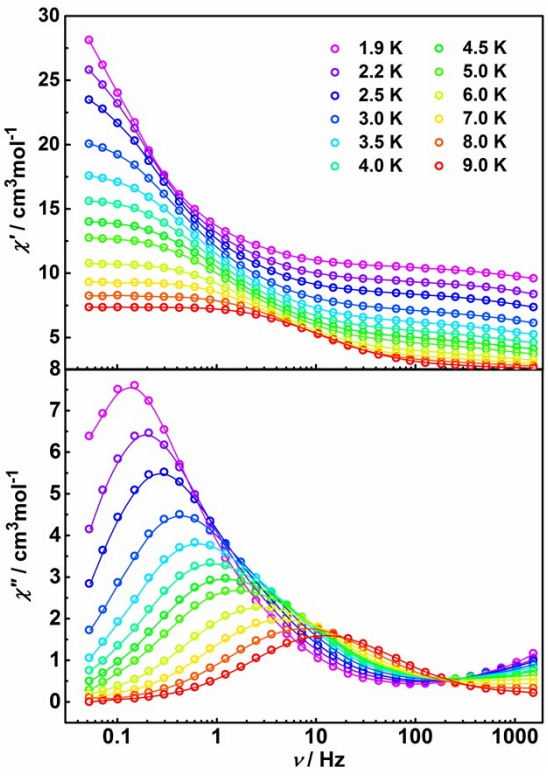

Fig. S5 Frequency dependence of the in-phase (χ') and out-of-phase (χ'') ac susceptibility signals between 1.9−9 K for **Dy_6−SCN** under zero dc-field. The solid lines represent fitting of the experimental data at different temperatures using sum of two modified Debye functions based on two relaxation progresses.

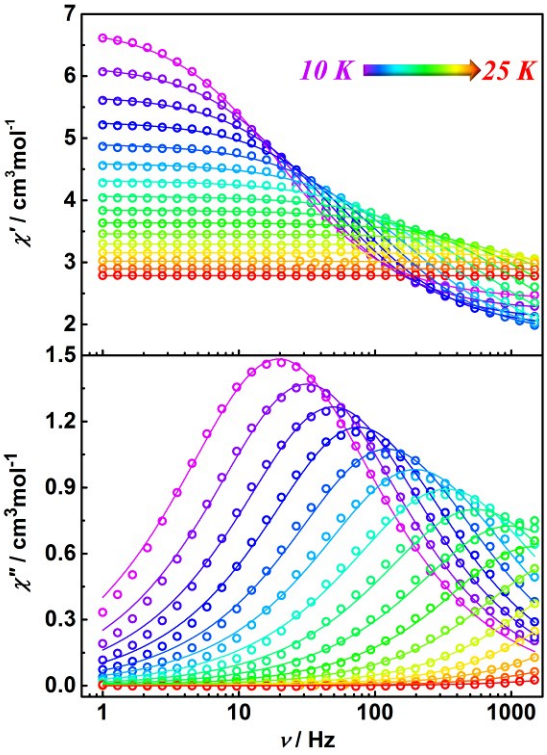

Fig. S6 Frequency dependence of the in-phase (χ') and out-of-phase (χ'') ac susceptibility signals between 10−25 K for **Dy_6−SCN** under zero dc-field. The solid lines represent fitting of the experimental data at different temperatures using the generalized Debye model.

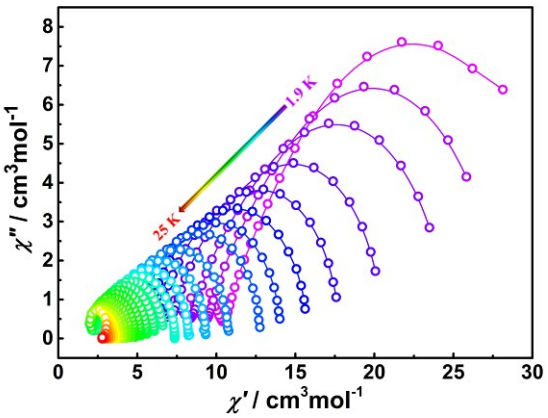

Fig. S7 Cole−Cole plots for temperatures between 1.9 and 25 K for **Dy_6−SCN** under a zero dc field. The Solid lines are guide for eyes.

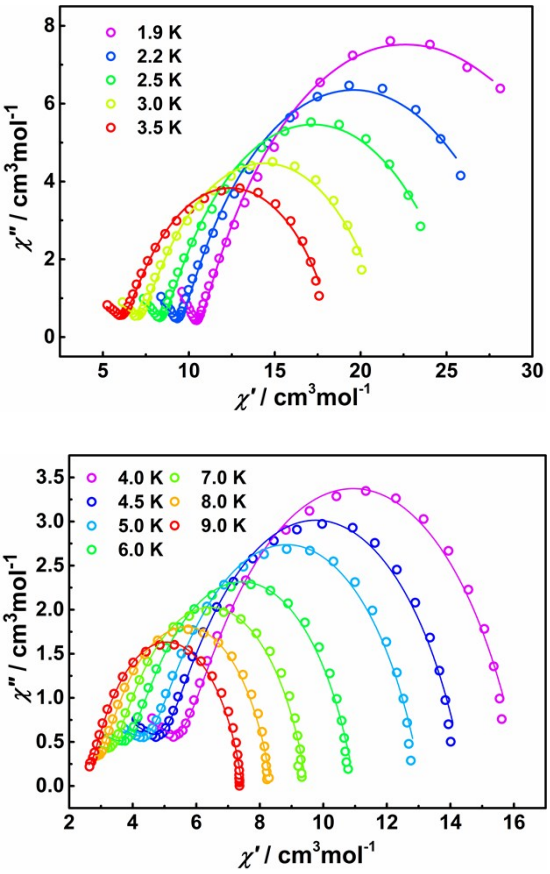

Fig. S8 Cole−Cole plots for temperatures between 1.9−3.5 and 4−9 K under a zero dc field with the best fit to the sum of two modified Debye functions based on two relaxation progresses for **Dy_6−SCN**. The Solid lines represent fits to the data, as described in the main text.

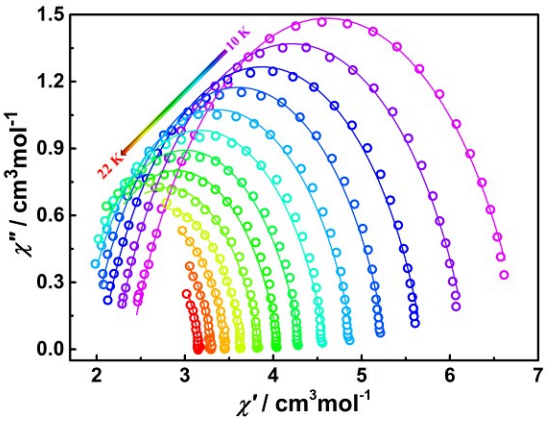

Fig. S9 Cole−Cole plots for temperatures between 10−22 K under a zero dc field with the best fit to the generalized Debye model for **Dy_6−SCN**. The Solid lines represent fits to the data, as described in the main text.

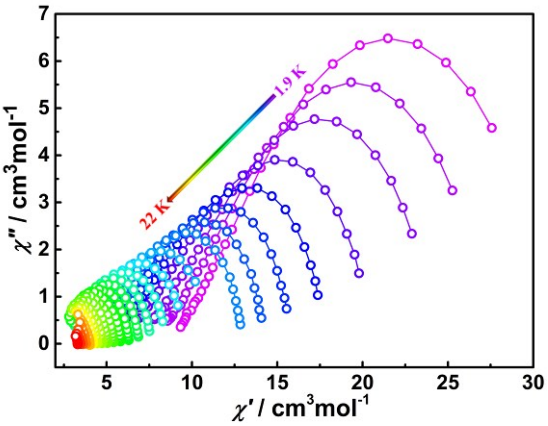

Fig. S10 Cole−Cole plots for temperatures between 1.9 and 22 K for **Dy_6−NO_3** under a zero dc field. The Solid lines are guide for eyes.

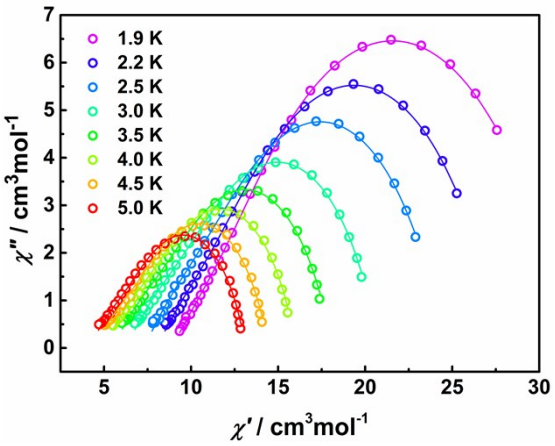

Fig. S11 Cole−Cole plots for temperatures between 1.9−5 K under a zero dc field with the best fit to the generalized Debye model for **Dy_6−NO_3**. The Solid lines represent fits to the data, as described in the main text.

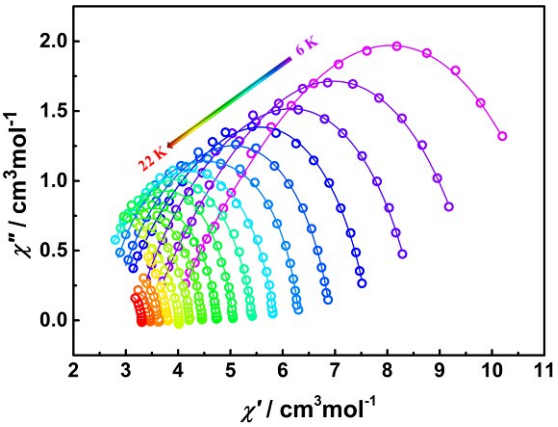

Fig. S12 Cole−Cole plots for temperatures between 6−22 K under a zero dc field with the best fit to the generalized Debye model for **Dy_6−NO_3**. The Solid lines represent fits to the data, as described in the main text.

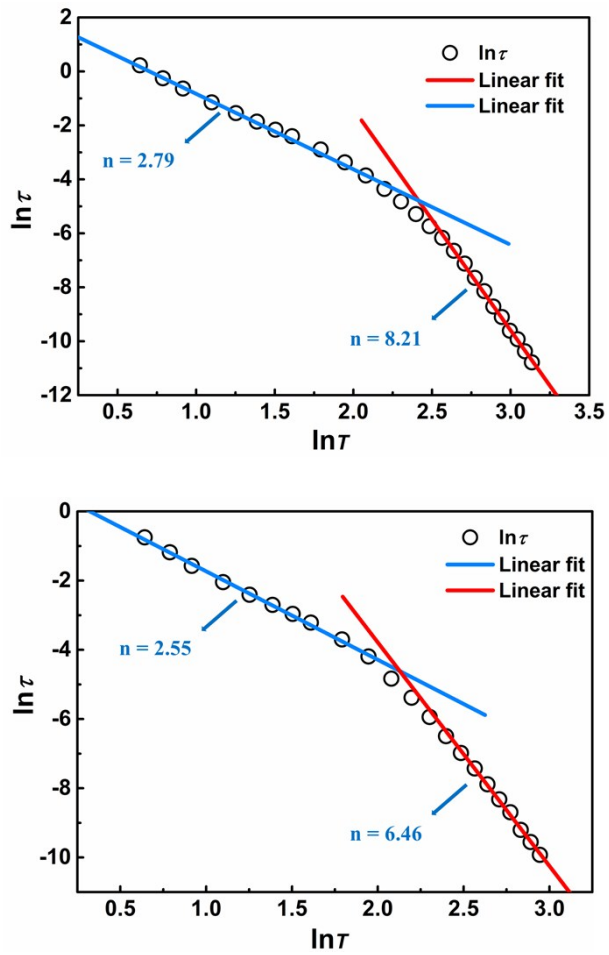

Fig. S13 Plot of lnτ versus ln$T$ for complexes **Dy_6−SCN** (top) and **Dy_6−NO_3** (bottom) under zero dc field. The solid lines are linear fitting results.

Table S5. Relaxation fitting parameters for Cole-Cole plots of **Dy_6−SCN** at varying temperatures under zero applied dc-field using the sum of two modified Debye model.[3]

T (K)	$\chi_{S,tot}$	$\Delta\chi_1$	$\Delta\chi_2$	α_1	α_2
1.9	0.902E-10	10.7	23.9	0.485	0.282
2.2	0.269E-09	9.76	19.7	0.577	0.270
2.5	0.297E-09	8.76	17.1	0.580	0.274
3.0	0.489E-09	7.51	14.0	0.595	0.277
3.5	0.834E-09	6.58	11.9	0.596	0.275
4.0	0.108E-08	5.88	10.4	0.602	0.273
4.5	0.159E-08	5.32	9.17	0.597	0.267
5.0	0.255E-08	4.93	8.18	0.615	0.260
6.0	0.235E-08	4.17	6.82	0.595	0.252
7.0	0.527E-08	3.65	5.82	0.600	0.237
8.0	0.188E-07	3.16	5.20	0.578	0.233
9.0	0.499E-08	2.78	4.66	0.575	0.224

Table S6. The best fitting parameters for Cole-Cole plots of **Dy_6−SCN** at varying temperatures under zero applied dc field.

T (K)	χ_T	χ_S	α
10	6.833	2.383	0.249
11	6.207	2.204	0.233
12	5.702	2.046	0.226
13	5.280	1.925	0.220
14	4.915	1.808	0.227
15	4.602	1.737	0.232
16	4.319	1.686	0.239
17	4.067	1.748	0.228
18	3.842	1.756	0.224
19	3.638	1.934	0.186
20	3.458	2.001	0.165
21	3.295	2.208	0.115
22	3.151	2.289	0.0757

Table S7. The best fitting parameters for Cole-Cole plots of **Dy_6−NO_3** at varying temperatures under zero applied dc field.

T (K)	χ_T	χ_S	α
1.9	34.5	9.62	0.409
2.2	30.2	8.74	0.421
2.5	26.5	7.93	0.427
3.0	22.2	6.91	0.431
3.5	19.1	6.16	0.428
4.0	16.8	5.59	0.419
4.5	15.0	5.12	0.409
5.0	13.6	4.76	0.396
6.0	12.0	4.03	0.424
7.0	10.1	3.60	0.389
8.0	8.76	3.26	0.358
9.0	7.79	2.99	0.331
10	7.01	2.81	0.306
11	6.39	2.58	0.291
12	5.88	2.44	0.279
13	5.45	2.42	0.254
14	5.08	2.35	0.239
15	4.76	2.33	0.242
16	4.47	2.34	0.227
17	4.23	2.26	0.228
18	4.02	2.29	0.219
19	3.80	1.93	0.252
20	3.62	2.86	0.137
21	3.47	2.95	0.151
22	3.31	2.88	0.127

References

1 V. P. K. M. B. Bushuev, N. V. Semikolenova, Yu. G. Shvedenkov,L. A., G. G. M. Sheludyakova, L. G. Lavrenova, V. A. Zakharov, and S. V. and Larionov, *Russ. J. Coord. Chem.*, 2007, **33**, 601.

2 (a) G. M. Sheldrick, *Acta Crystallogr. A*, 2008, **64**, 112; (b) O. V. Dolomanov, L. J. Bourhis, R. J. Gildea, J. A. K. Howard and H. Puschmann, *J. Appl. Crystallogr.*, 2009, **42**, 339.

3 Y.-N. Guo, G.-F. Xu, Y. Guo and J. Tang, *Dalton Trans.*, 2011, **40**, 9953.